

# Formation UAV Flight Control using Virtual Structure and Motion Synchronization

Norman H. M. Li and Hugh H. T. Liu

**Abstract**—In this paper, the synchronized position tracking controller is incorporated in formation flight control for multiple flying wings. With this technology, the performance and effectiveness of the formation controller are improved when the virtual structure approach is utilized to maintain formation geometry. Simulations are conducted on the nonlinear model of two flying wings to verify the proposed controller.

## I. INTRODUCTION

Formation flight control of multiple Unmanned Aircraft Vehicles (UAVs) has been an active research topic for many years [1], [2], [3], [4] since it promises many practical applications, such as reconnaissance, surveillance, atmospheric study, communication relaying and search and rescue. Some of these tasks may be dangerous and will not be recommended for human pilots, thus making them ideal for autonomous unmanned vehicles.

There are basically three approaches to the formation control problem for multiple vehicles, namely leader following, behavioral, and virtual structure [5], [6], [7]. In the virtual structure approach used in this paper, the entire formation is treated as a single entity. It can evolve as a rigid body in a given direction with some given orientation and maintain the geometric relationship among multiple vehicles base on a reference point in the virtual structure. As for the more specific formation flight problem for aircraft, a consensus is that the vehicles should be able to achieve tracking for given velocity, heading, and altitude commands ([1], [2], [8], [9]) in order for a formation controller to be developed for the aircraft. An autopilot model that provides tracking capabilities for the three commands and the method of trajectory command modifications based on relative position errors is used as part of the control algorithm in our paper. This method is coupled with the virtual structure approach to achieve formation flights for our research.

In this paper, we present that the performance of a formation controller using certain virtual structure definitions can be enhanced by applying the synchronization technology developed by UTIAS [4], [10]. The technology synchronizes the relative position tracking motion between multiple aircraft. Simulation results demonstrate the effectiveness and performance improvement with the proposed control method.

The remainder of this paper is organized as follows. In Section II, the virtual structure is defined followed by the

formation algorithm development in Section III. In Section IV, the synchronization technology is incorporated into the controller. Simulation results on formation control of multiple flying wings are given in Section V. Finally, Section VI offers conclusions and future research possibilities.

## II. VIRTUAL STRUCTURE

In the virtual structure approach, the entire formation is treated as a rigid body. The positions of the vehicles in the structure are usually defined in a frame with respect to a reference point in the structure. As a trajectory is given for the reference point, the desired position for each vehicle can be calculated as the virtual structure evolves in time. In our formation controller, we define the centroid of the desired formation as the reference point in the virtual structure.

From [7], defining frame  $O$  is an inertial frame and frame  $F$  is the formation reference frame located at the reference point. The formation is a rigid body with inertial position  $P_F$ , velocity  $V_F$ , heading  $\psi_F$ , and angular velocity  $\omega_F$ . We also have the reference frame  $i$  imbedded in each agent. Each agent can be represented by position  $P_i$ , velocity  $V_i$ , heading  $\psi_i$  and angular velocity  $\omega_i$  with respect to the inertial frame  $O$  or by  $P_{iF}$ ,  $V_{iF}$ ,  $\psi_{iF}$  and  $\omega_{iF}$  with respect to the formation reference frame  $F$ . Then the equations for the position and velocity dynamics for each agent in the inertial frame in the virtual structure are

$$\begin{aligned} P_i^d(t) &= P_F(t) + C_{OF}(t) P_{iF}^d(t) \\ V_i^d(t) &= V_F(t) + C_{OF}(t) V_{iF}^d(t) \\ &\quad + \omega_F(t) \times (C_{OF}(t) P_{iF}^d(t)) \end{aligned} \quad (1)$$

where  $C_{OF}(t)$  denotes the rotation matrix from frame  $F$  to frame  $O$  and variables with superscript  $d$  represent the desired values of the variables for the corresponding vehicle.

Consider the case with two vehicles UAV1 and UAV2, assuming each vehicle is fixed in the virtual structure, then  $V_{iF}^d(t) = 0$  in (1). In the two vehicles case,  $P_{2F}^d(t) = -P_{1F}^d(t)$  if the reference point is defined to be the centroid of the entity. Therefore, defining  $\Gamma(t) = C_{OF}(t) P_{1F}^d(t)$ , equation (1) for UAV1 becomes

$$\begin{aligned} P_1^d(t) &= P_F(t) + \Gamma(t) \\ V_1^d(t) &= V_F(t) + \omega_F(t) \times \Gamma(t) \end{aligned} \quad (2)$$

and for UAV2, by substitutions of  $P_{2F}^d(t)$  and  $\Gamma(t)$ ,

$$\begin{aligned} P_2^d(t) &= P_F(t) - \Gamma(t) \\ V_2^d(t) &= V_F(t) - \omega_F(t) \times \Gamma(t) \end{aligned} \quad (3)$$

Also, at the time instant  $t = t_0$  where there is a non-zero  $\omega_F(t_0)$ , the instantaneous attitude changes required for the

N. Li is with The Institute for Aerospace Studies, University of Toronto, 4925 Dufferin Street, Toronto, Canada M3H 5T6 norman.li@utoronto.ca

H. Liu is with The Institute for Aerospace Studies, University of Toronto, 4925 Dufferin Street, Toronto, Canada M3H 5T6 liu@utias.utoronto.ca

aircraft in order to maintain the geometry (not the attitude of the vehicles alone) will be opposite, as shown in Fig. 1 with  $\omega_F(t_0)$  being about the  $z$ -axis for an example.

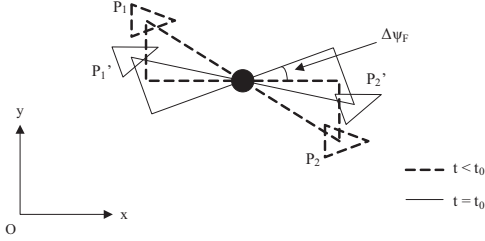


Fig. 1: Change in UAVs' headings

For the UAVs to go from  $P_i$  to  $P_i'$ , UAV1's instantaneous heading change will be in the direction of  $-\Delta\psi_F(t_0)$  with a larger magnitude; while UAV2's heading change will be in the direction of  $\Delta\psi_F(t_0)$  with a larger magnitude. Therefore,

$$\begin{aligned}\Delta\psi_1^d(t_0) &= -(1 + \kappa_1) \Delta\psi_F(t_0) \\ \Delta\psi_2^d(t_0) &= (1 + \kappa_2) \Delta\psi_F(t_0)\end{aligned}\quad (4)$$

with  $\kappa_i > 0$  as a constant. The same analogy can be applied to the roll ( $\Delta\phi$ ) and pitch ( $\Delta\theta$ ) attitude changes.

Base on the desired positions  $P_i^d$ , velocities  $V_i^d$  and heading changes  $\Delta\psi_i^d$  of the two vehicles in (2-4), it can be observed that the relative values for each vehicle are opposite in magnitude with respect to the reference point  $P_F$  when it is the centroid of the virtual structure. Thus, it should be expected that the relative position errors, if there are any, between the actual vehicles' positions and the reference point will be opposing in nature as well when the same trajectory command designated for the reference point is given to both vehicles. Simulation results in Section V verify this hypothesis. Therefore, a controller should be developed to eliminate these position errors for the vehicles to maintain formation.

### III. FORMATION CONTROL ALGORITHM

To eliminate the relative position errors and to keep the vehicles in formation geometry during flight, a formation controller is needed. It is typically implemented by a two loop scheme where the inner control allows tracking of commanded velocity ( $V$ ), heading ( $\psi$ ) and altitude ( $H$ ). In the outer loop, the formation controller generates the reference commands for the inner controller. An autopilot that is capable of tracking velocity, altitude and heading is used in our paper, so we focus the development on the outer loop formation controller.

Base on the reference trajectory commands  $T_r = [V_r, \psi_r, H_r]^T$  for the reference point  $P_r = [x_r, y_r, z_r]^T$  and the defined relative distances in the virtual structure, the desired position for each vehicle during the flight  $P_i^d = [x_i^d, y_i^d, z_i^d]^T$  can be calculated, whereas the actual position of each aircraft  $P_i = [x_i, y_i, z_i]^T$  can be obtained from the GPS system located on the vehicle. Using the reference trajectory and the actual/desired positions for the vehicles as input, the

formation controller generates the modified trajectories for each UAV to maintain the geometry of the formation during the flight. We define the relative position errors for the  $i^{th}$  vehicle during the flight in the inertial frame as

$$\begin{bmatrix} e_{xi} \\ e_{yi} \\ e_{zi} \end{bmatrix} = \begin{bmatrix} x_i^d - x_i \\ y_i^d - y_i \\ z_i^d - z_i \end{bmatrix}\quad (5)$$

To utilize these relative errors in (5), they need to be converted into errors in the formation frame using the rotation matrix  $C_{FO}(t) = C_{OF}(t)^{-1}$ . Therefore,

$$\begin{bmatrix} e_{xiF} \\ e_{yiF} \\ e_{ziF} \end{bmatrix} = C_{FO}(t) \begin{bmatrix} e_{xi} \\ e_{yi} \\ e_{zi} \end{bmatrix}\quad (6)$$

The modified trajectory command for the inner loop controller is  $T_{ci} = T_r + \Delta T_i$ , where  $\Delta T_i$  is calculated through a PI controller based on the relative position errors in (6).

$$\begin{aligned}\Delta V_i(t) &= K_{px} e_{xiF}(t) + K_{ix} \int_0^t e_{xiF}(t) dt \\ \Delta \psi_i(t) &= K_{py} e_{yiF}(t) + K_{iy} \int_0^t e_{yiF}(t) dt \\ \Delta H_i(t) &= K_{pz} e_{ziF}(t) + K_{iz} \int_0^t e_{ziF}(t) dt\end{aligned}\quad (7)$$

$$\Delta T_i = \begin{bmatrix} \Delta V_i(t) \\ \Delta \psi_i(t) \\ \Delta H_i(t) \end{bmatrix}\quad (8)$$

The formation controller applies the corrected trajectory commands  $T_{ci}$  based on  $T_r$  and  $\Delta T_i$  in (8) to the aircraft's autopilots. These corrections account for the changes required to maintain the geometry of the formation. Simulation results of the controller are shown in Section V in this paper.

### IV. RELATIVE POSITION SYNCHRONIZATION

One of the objectives in our project is to incorporate the motion synchronization technology in our design to achieve coordinated control of the UAVs. Thus, the next step is to apply this technology in our controller.

The strategy uses the cross coupling concept to synchronize the relative position tracking motion of the aircraft. It utilizes synchronization errors  $\varepsilon_i$ , which incorporate error information from different agents in the system, to identify the performance of the synchronization. The cross coupled error  $e_i^*$  then couples the error  $e_i$  and synchronization error  $\varepsilon_i$  through a positive synchronization gain  $\beta_i$ .

$$e_i^* = e_i + \beta_i \varepsilon_i\quad (9)$$

The objective of the synchronization strategy is to drive  $e_i^*$  of each agent in (9) to 0 by choosing the proper gain values, implying that both  $e_i$  and  $\varepsilon_i$  are driven to 0 as well. In order words, the vehicles are using information from each other to eliminate the errors synchronously.

In our case of two vehicles, the position synchronization errors are defined as

$$\begin{aligned} \varepsilon_{x1F} &= e_{x1F} - e_{x2F}, & \varepsilon_{x2F} &= e_{x2F} - e_{x1F} \\ \varepsilon_{y1F} &= e_{y1F} - e_{y2F}, & \varepsilon_{y2F} &= e_{y2F} - e_{y1F} \\ \varepsilon_{z1F} &= e_{z1F} - e_{z2F}, & \varepsilon_{z2F} &= e_{z2F} - e_{z1F} \end{aligned} \quad (10)$$

Then the coupled position errors are formed to include both the position tracking errors  $e_i$  and the position synchronization errors  $\varepsilon_i$  from (10)

$$\begin{aligned} e_{xiF}^* &= e_{xiF} + \beta_{xi}\varepsilon_{xiF} \\ e_{yiF}^* &= e_{yiF} + \beta_{yi}\varepsilon_{yiF} \\ e_{ziF}^* &= e_{ziF} + \beta_{zi}\varepsilon_{ziF} \end{aligned} \quad (11)$$

where  $\beta_{xi}$ ,  $\beta_{yi}$ , and  $\beta_{zi}$  in (11) are positive synchronization gains for the  $x$ ,  $y$ , and  $z$  channels of the  $i^{th}$  aircraft. The method of coupling the errors in (10) can vary when more than two vehicles are involved to couple errors from more than one aircraft, as introduced in [10].

The coupled relative position errors from (11) are used to calculate the trajectory modification  $\Delta T_i^*$  and the new modified trajectory command that will be passed to the inner controller of the vehicles is  $T_{ci}^* = T_r + \Delta T_i^*$  where

$$\begin{aligned} \Delta V_i^*(t) &= K_{px}e_{xiF}^*(t) + K_{ix} \int_0^t e_{xiF}^*(t) dt \\ \Delta \psi_i^*(t) &= K_{py}e_{yiF}^*(t) + K_{iy} \int_0^t e_{yiF}^*(t) dt \\ \Delta Z_i^*(t) &= K_{pz}e_{ziF}^*(t) + K_{iz} \int_0^t e_{ziF}^*(t) dt \end{aligned} \quad (12)$$

$$\Delta T_i^* = \begin{bmatrix} \Delta V_i^*(t) \\ \Delta \psi_i^*(t) \\ \Delta Z_i^*(t) \end{bmatrix} \quad (13)$$

The synchronization strategy is implemented as proposed with the same setup as previous models. Simulation results are shown in Section V in this paper.

To show that the concept of synchronized position will improve the performance of the formation controller, consider the coupled errors  $e_{x1F}^*$  and  $e_{x2F}^*$  in two cases.

*Case 1:* The relative position errors are opposite in magnitude as proposed in Section II, then

$$e_{x1F} = -\eta e_{x2F} \quad \eta > 0 \quad (14)$$

Substituting (14) in the calculation of the coupled errors (10), the synchronization error terms become the following.

$$\varepsilon_{x1F} = e_{x1F} - e_{x2F} = \left(1 + \frac{1}{\eta}\right) e_{x1F} \quad (15)$$

$$\varepsilon_{x2F} = e_{x2F} - e_{x1F} = (1 + \eta) e_{x2F} \quad (16)$$

Using (15) and (16), the coupled position errors of the vehicles can be derived from (11).

$$e_{x1F}^* = \left[1 + \left(1 + \frac{1}{\eta}\right) \beta_{x1}\right] e_{x1F} \quad (17)$$

$$e_{x2F}^* = [1 + (1 + \eta) \beta_{x2}] e_{x2F} \quad (18)$$

Since  $\beta_{xi} > 0$  by definition and  $\eta > 0$ , therefore  $|e_{xiF}^*| > |e_{xiF}|$  from (17) and (18). This causes the controller to correct the velocity command in (12) in a faster manner with the same PI gains as  $|\Delta V_i^*| > |\Delta V_i|$ , thus eliminating  $e_{xiF}$  faster and in turn eliminates the synchronized error  $\varepsilon_{xiF}$  as well. In conclusion, the vehicles correct their trajectories quicker by using the coupled errors to improve the performance of the controller.

*Case 2:* The relative position errors has the same sign as each other, then (14) becomes

$$e_{x1F} = -\eta e_{x2F} \quad \eta < 0 \quad (19)$$

From  $\beta_{xi} > 0$  and  $\eta < 0$ , derivations from (17), (18) will result in  $|e_{x1F}^*| > |e_{x1F}|$  and  $|e_{x2F}^*| < |e_{x2F}|$  or vice versa by having  $\eta$  in reciprocal terms in the equations.

In the case of  $|e_{xiF}^*| > |e_{xiF}|$ , the coupling strategy again has the effect of eliminating  $e_{xiF}$  faster. However, in the case of  $|e_{xiF}^*| < |e_{xiF}|$ , the correction of  $e_{xiF}$  will be slower. This is the scenario where one of the vehicles is sacrificing its own performance to maintain the formation geometry better with other vehicles in the system as a whole. Therefore, the robustness of the formation flight is increased by the coupling and synchronizing behavior between the aircraft.

One possible worst case scenario from Case 2 is when  $|e_{xiF}^*| = -\delta_1 |e_{xiF}|$  and  $\delta_1 > 0$ , resulting in opposite correction taken by one vehicle when calculating trajectory modification, but this scenario will eventually evolve to  $|e_{xiF}^*| = \delta_2 |e_{xiF}|$  and  $\delta_2 > 0$  as the other vehicle is eliminating its own error in the proper way.

Concluding results from both cases, the performance of the formation controller will improve with the incorporation of the synchronization technology. Simulations have been conducted with both cases and improvements are evident.

## V. SIMULATIONS

Simulations are performed on a circular maneuver followed by straight line travel for two UAVs in a level flight formation, thus we focus on the commands and responses related to the  $xy$ -plane. An autopilot model, using the same architecture as the one in [11], developed for a MAGICC lab flying wing UAV, is used in the simulations. The desired relative distances from UAV1 and UAV2 to the reference point in the virtual structure are defined as  $[-4, 4, -1]^T m$  and  $[4, 4, 1]^T m$  respectively. The UAVs start at the desired positions at the beginning of the flight. A velocity of  $14m/s$  and a heading rate of  $2^\circ/s$  are applied to the reference point. No collision avoidance algorithm is implemented.

Fig. 2(a) and Fig. 3(a) illustrate the relative position errors and the trajectories of the aircraft and the reference point with no formation control. It can be seen that the formation flight is not achieved and the relative position errors are opposite in magnitude when the reference point is defined as the centroid in the virtual structure as proposed in Section II.

Formation control is then implemented for the UAVs based on virtual structure approach and trajectory modifications

as proposed in Section III. The setup for the simulation is the same as before and the gains used for the trajectory PI controllers are given in Table I.

TABLE I: Control Gains of PI Controller

Parameters	Values	Parameters	Values
$K_{px}$	5	$K_{ix}$	0.5
$K_{py}$	0.005	$K_{iy}$	0.0005
$K_{pz}$	1	$K_{iz}$	0.005

Fig. 2(b) and Fig. 3(b) show the simulation results with formation controller implemented. It can be seen that the vehicles now maintain formation during flight and the relative position errors are stabilizing around zero, although there are obvious differences between the errors from the two aircraft.

Finally, the synchronization technology in Section IV is incorporated in the controller. The synchronization gains  $\beta_{xi}$ ,  $\beta_{yi}$ , and  $\beta_{zi}$  for both vehicles are being set to 1. In this case, simulation results in Fig. 2(c) and Fig. 3(c) show that formation flight is again achieved between the two vehicles and the relative position errors in the virtual structure stabilize around zero. In comparison to Fig. 2(b), the relative position errors for the UAVs have been reduced.

A quantitative index that can be used to measure the performance of the controller is the root mean square (rms) value of the errors. Using the relative position error data from the two vehicles, their error root mean square values ( $E_{rms}$ ) in the  $x$  and  $y$  directions for the three simulation scenarios (No. 1, 2 and 3) are summarized into Table II.

TABLE II: Relative position error rms ( $E_{rms}$ ) of UAVs

UAV1			
No.	Formation control method	$E_{rms}$ in $x$	$E_{rms}$ in $y$
1	None (using reference commands)	7.5308m	5.5214m
2	Trajectory commands modification	0.0951m	1.0931m
3	No.2 with synchronization	0.0427m	0.4322m
UAV2			
No.	Formation control method	$E_{rms}$ in $x$	$E_{rms}$ in $y$
1	None (using reference commands)	7.5000m	5.5445m
2	Trajectory commands modification	0.0888m	1.0016m
3	No.2 with synchronization	0.0354m	0.5552m

The large  $E_{rms}$  values for the two vehicles in the  $x$  and  $y$  directions with no formation algorithm corresponds to the formation being broken. When the formation controller is used, the  $E_{rms}$  values in the  $x$  and  $y$  directions decrease by a significant amount. The decrease in the error rms values indicates that the vehicles are trying to maintain formation. The values further decrease when the synchronization strategy is incorporated. As an example, take the UAV1  $E_{rms}$  value in  $x$  from Table II, it is shown that the  $E_{rms}$  from using the trajectory commands modification controller without synchronization strategy is 0.0951m, however, the error is reduced to 0.0427m with synchronization strategy. Using the error without synchronization as the nominal value, this corresponds to a  $(0.0951 - 0.0427)/0.0951 * 100\%$

$= 55.1\%$  decrease. Similar calculations reveal the same improvements in the  $E_{rms}$  value in  $y$  and also the  $E_{rms}$  values for UAV2 (approximately 50%). This demonstrates that the strategy improves the performance of the formation controller. In other words, the vehicles maintain the virtual structure formation in a more “synchronized” pattern.

## VI. CONCLUSIONS AND FUTURE WORK

In conclusion, by adapting motion synchronization to the relative distance errors from the UAVs, the formation is being kept better by the vehicles. Simulations have also been conducted on non-level flights and UAVs starting in different initial positions, the results are acceptable as formation is again kept with the controller. This technique can be easily expanded to more than two vehicles as long as the relative distances of each UAV from the reference point are defined.

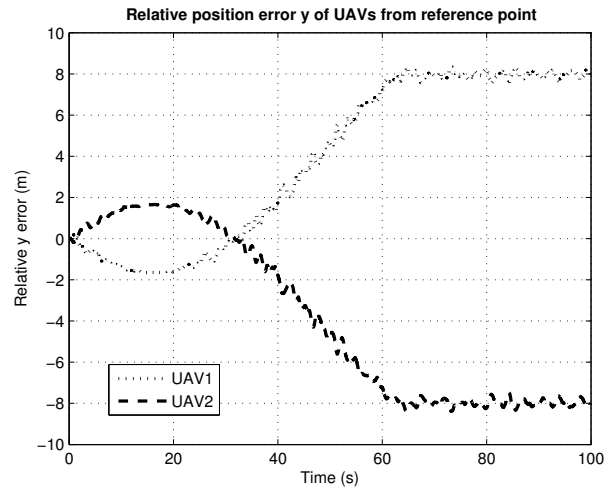
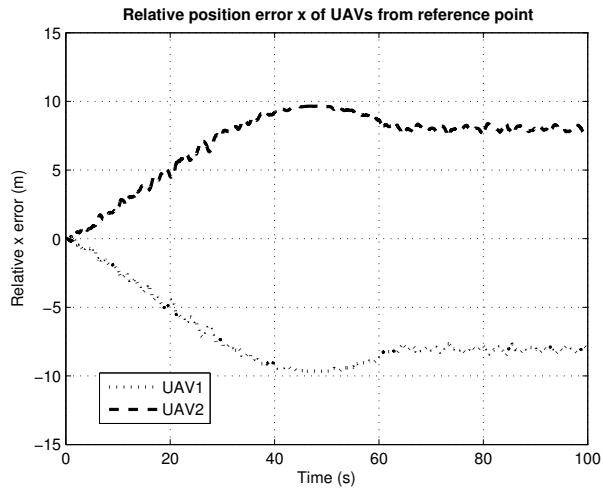
Future work includes reconfiguration of the virtual structure if the relative distances are defined as functions of time during formation flight. Investigation can also be performed on centralized/decentralized approaches for more than two aircraft. At UTIAS, implementation on real vehicles to verify the proposed controller in this paper is currently being undertaken and flight tests will be performed to study the effectiveness and performance of the controller.

## VII. ACKNOWLEDGMENTS

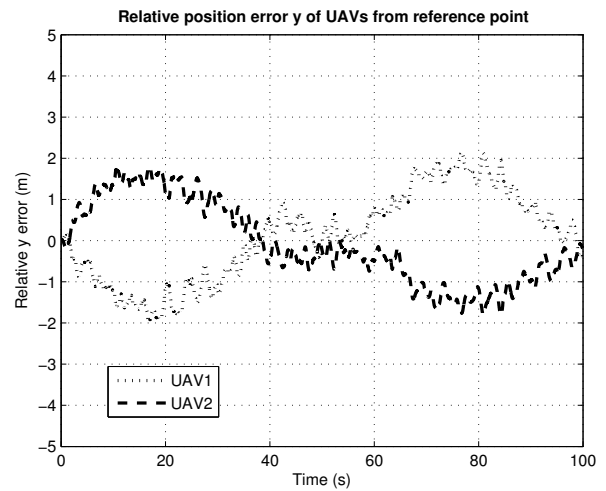
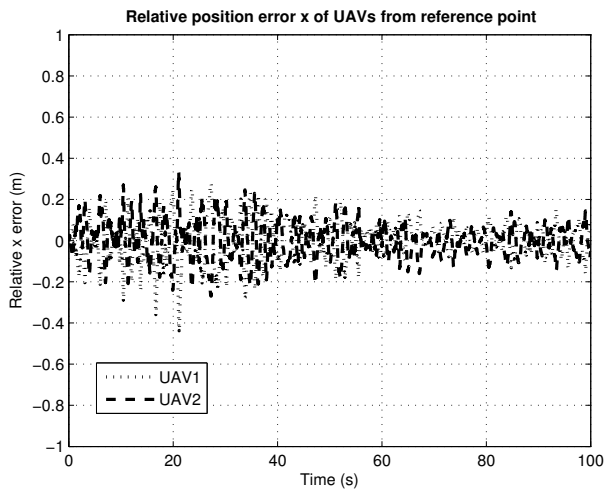
The authors gratefully acknowledge Ruben Perez for his contribution to this work.

## REFERENCES

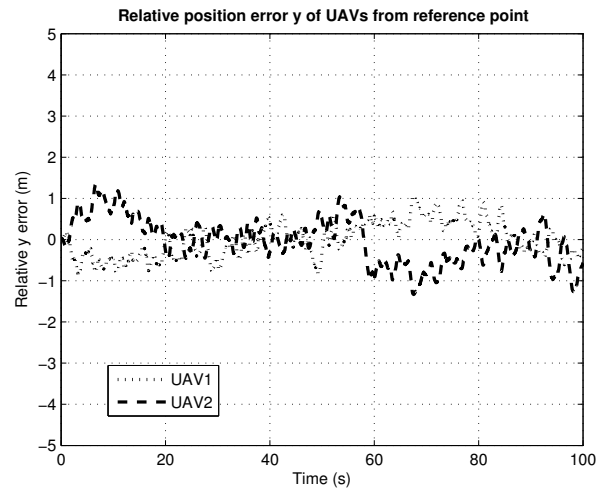
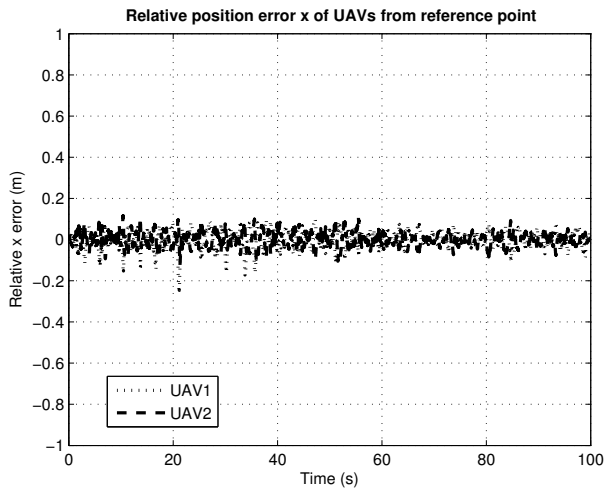
- [1] F. Giulietti, L. Pollini, and M. Innocenti, “Autonomous formation flight,” *IEEE Control Systems Magazine*, vol. 20, no. 6, pp. 34–44, 2000.
- [2] M. Pachter, J. J. D’Azzo, and A. W. Proud, “Tight formation flight control,” *Journal of Guidance, Control, and Dynamics*, vol. 24, no. 2, pp. 246–254, March–April 2001.
- [3] Y. Gu, B. Seanor, G. Campa, M. R. Napolitano, L. Rowe, S. Gururajan, and S. Wan, “Design and flight testing evaluation of formation control laws,” *IEEE Transactions on Control Systems Technology*, vol. 14, no. 6, pp. 1105–1112, 2006.
- [4] J. Shan and H. T. Liu, “Close-formation flight control with motion synchronization,” *Journal of Guidance, Control and Dynamics*, vol. 28, no. 6, pp. 1316–1320, November–December 2005.
- [5] J. R. T. Lawton, R. W. Beard, and B. J. Young, “A decentralized approach to formation maneuvers,” *IEEE Transactions on Robotics and Automation*, vol. 19, no. 6, December 2003.
- [6] B. J. Young, R. W. Beard, and J. M. Kelsey, “A control scheme for improving multi-vehicle formation maneuver,” in *American Control Conference*, Arlington, VA, June 25–27 2001, pp. 704–709.
- [7] W. Ren and R. W. Beard, “Virtual structure based spacecraft formation control with formation feedback,” in *AIAA Guidance, Navigation, and Control Conference and Exhibit*, Monterey, California, August 5–8 2002, AIAA Paper no. 2002-4963.
- [8] Y. D. Song, Y. Li, and X. H. Liao, “Orthogonal transformation based robust adaptive close formation control of multi-uavs,” in *American Control Conference*, Portland, OR, June 8–10 2005, pp. 2983–2988.
- [9] R. Kumar, P. T. Kabamba, and D. C. Hyland, “Controller design using adaptive random search for close-coupled formation flight,” *Journal of Guidance, Control, and Dynamics*, vol. 28, no. 6, pp. 1323–1325, November–December 2005.
- [10] J. Shan and H. H. T. Liu, “Synchronized tracking control of multiple flying wings,” in *American Control Conference*, Minneapolis, MN, June 14–16 2006, pp. 1434–1439.
- [11] W. Ren and R. W. Beard, “Trajectory tracking for unmanned air vehicles with velocity and heading rate constraints,” *IEEE Transactions on Control Systems Technology*, vol. 12, no. 5, pp. 706–716, September 2004.



(a) Relative positions errors of UAVs - No formation algorithm implemented

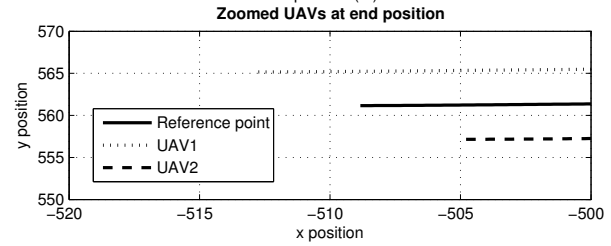
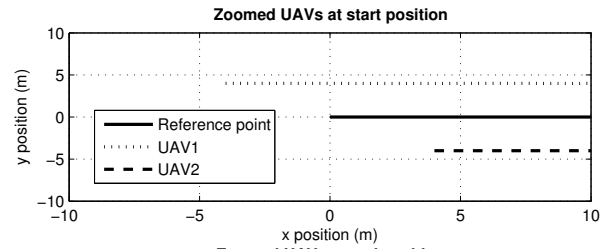
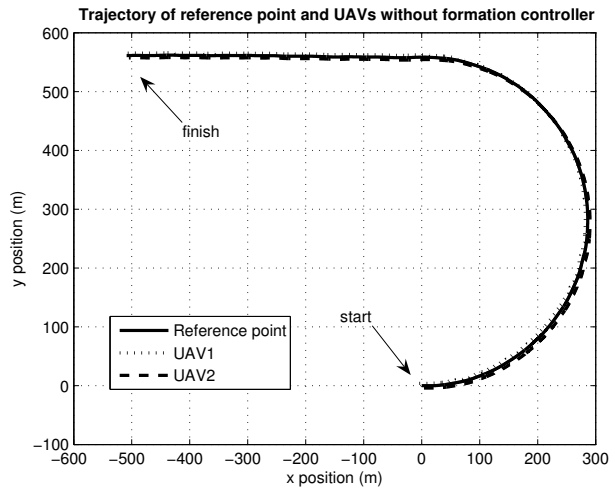


(b) Relative positions errors of UAVs - Trajectory commands modification

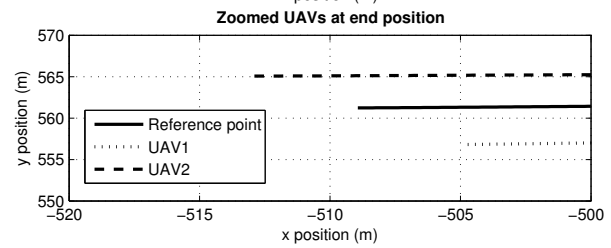
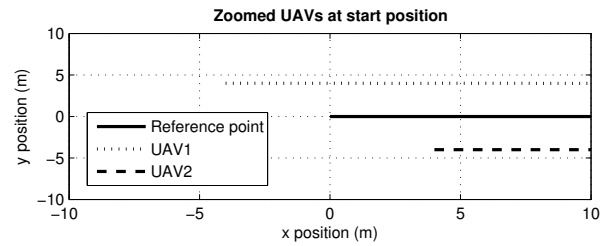
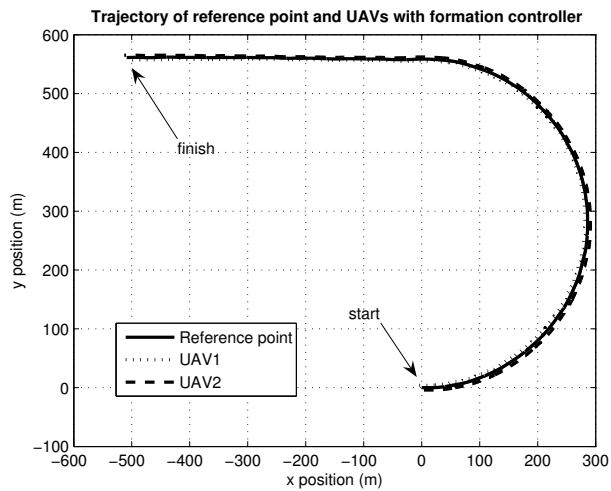


(c) Relative positions errors of UAVs - Trajectory commands modification with synchronization

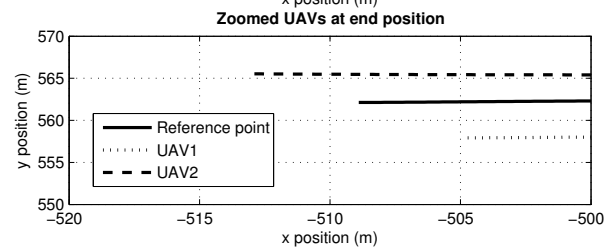
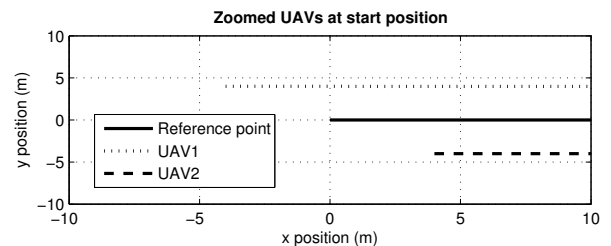
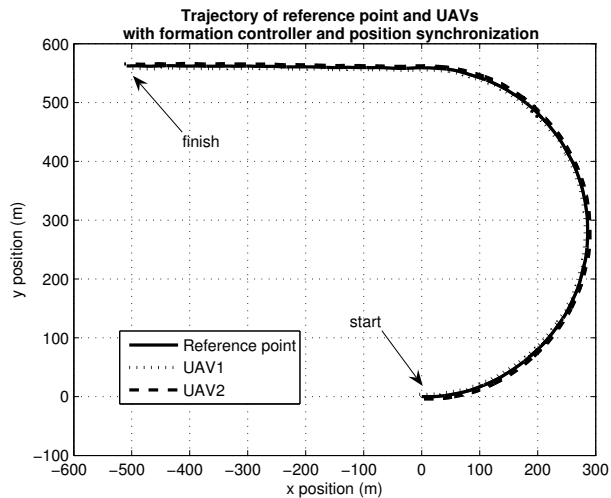
Fig. 2: Relative position errors of 2 flying wings in simulations



(a) Trajectory responses of UAVs - No formation algorithm implemented



(b) Trajectory responses of UAVs - Trajectory commands modification



(c) Trajectory responses of UAVs - Trajectory commands modification with synchronization

Fig. 3: Trajectory responses of 2 flying wings in simulations